Available online at www.sciencedirect.com
ScienceDirect
Journal of Asian Earth Sciences 29 (2007) 29–40
Journal of Asian Earth Sciences
www.elsevier.com/locate/jaes

Geochemistry and petrogenesis of spinel lherzolite xenoliths from Boeun, Korea

Young-Woo Kil *

Nano Material Team, Korea Basic Science Institute, 52 Yeoeun-Dong, Yusung-Gu, Daejeon 305-333, South Korea

Received 16 March 2005; received in revised form 16 August 2005; accepted 20 December 2005

Abstract

Geochemical characteristics of spinel lherzolite xenoliths, enclosed in Miocene alkali basalt from Boeun, Korea, provide important clues for understanding the lithosphere composition, equilibrium temperature and pressure conditions, and depletion and enrichment processes of subcontinental lithospheric mantle beneath Boeun. The spinel lherzolite xenoliths with protogranular to porpyroclastic textures were accidentally trapped by the ascending alkali basalt magma. The spinel lherzolite xenoliths originated at depths between 50 and 63 km with equilibrium temperatures ranging from 847 to 1030 °C. These xenoliths may have undergone small degrees (1–2%) of partial melting and cryptic metasomatism by an alkali basaltic melt. Based on Sr and Nd isotope compositions, the subcontinental lithospheric mantle beneath Boeun was heterogeneous and similar to that beneath East China and Central Mongolia rather than the Japanese Island Arc.

Keywords: Spinel lherzolite; Metasomatism; Lithospehric mantle; Geochemistry

1. Introduction and geological setting

Upper mantle xenoliths found in alkali basalts, kimberlites and lamprophyre clans provide important information on the chemical composition, mineralogy, and P–T conditions of the upper mantle (Maaløe and Aoki, 1977; Bonatti et al., 1986; Nixon, 1987; Witt-Eickschen and Seck, 1987; Zipfel and Wörner, 1992; Ho et al., 2000). Upper mantle xenoliths enclosed in Cenozoic alkali basalts in South Korea were found at Boeun, Gangseong, Baegryeong Isalnd, and Jeju lsalnd (Kim et al., 1988; Choi, 2000; Choi et al., 2001, 2002; Lee, 2002). Boeun is located in the Ogcheon belt of central South Korea (Fig. 1). The ultramafic xenoliths found there have not been studied in detail (Kim et al., 1988; Lee, 2002).

The Korean peninsula is part of the Amuria Plate, providing an important link between the continental blocks of North and South China and the island arcs of Japan. The geology of Korea can be divided into seven tectonic zones that are, from north to south: the Nangrim massif, the Pyeongnam basin, the Imjingang belt, the Gyeonggi massif, the Ogcheon belt, the Yeongnam massif, and the Gyeongsan basin. The Ogcheon belt is a NE-trending fold and thrust belt, bounded by the Gyeonggi massif and the Yeongnam massif (Cluzel et al., 1991; Chough et al., 2000). An alkali basalt flow with a diameter of about 300 m is distributed in Boeun within the central Ogcheon belt. The alkali basalt, with an age of 11.1 Ma as dated by the K–Ar method, contains spinel lherzolite xenoliths (up to 10 cm) (Kim et al., 2004).

In this paper, I present the mineral chemistry and isotopic compositions of the spinel lherzolites and try to deduce the equilibrium temperature and pressure conditions of the xenoliths along with the deep geological processes in the subcontinental lithospheric mantle (SCLM) beneath Boeun. The chemical characteristics of SCLM beneath

* Present address: New Ventures, Korea National Oil Corporation, 1588-14, Gwanyang-dong, Dongan-gu, Anyang Gyunggi-do 431-711, South Korea. Tel.: +82 3 138 025 76; fax: +82 3 138 412 75.
E-mail address: ykil@knoc.co.kr.

1367-9120/$ - see front matter © 2006 Elsevier Ltd. All rights reserved.
doi:10.1016/j.jseaes.2005.12.006

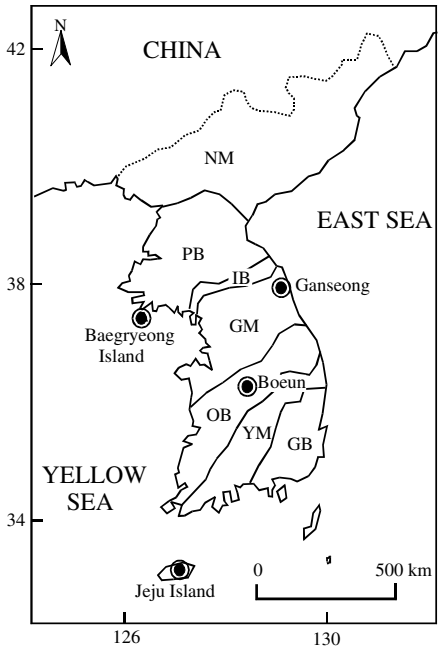

Fig. 1. Simplified tectonic map showing the sampling location at Boeun and mantle xenolith sites in Korea. NM, Nangrim massif; PB, Pyeongnam basin; IB, Imjingang belt; GM, Gyeonggi massif; OB, Ogcheon belt; YM, Yeongnam massif; GB, Gyeongsang basin.

Boeun will be compared with those beneath East China and Southeast Japan in order to determine their geological significance.

2. Analytical method

Nine spinel lherzolites were selected by microscope for petrographic characterization. The modal composition of spinel lherzolite was determined by point counting using a variable grid spacing to minimize counting error as outlined by Solomon (1963). The total number of point counts is about 1300 and the measured area of the thin section is 750 mm^2.

Analyses of mineral chemistry were carried out with a Cameca SX-51 microprobe at the Korea Basic Science Institute (KBSI) with wavelength dispersive mode. Olivine, orthopyroxene and clinopyroxene grains were hand-picked under a binocular microscope and analyzed separately, and the fine-grained spinels were analyzed in thin section.

Except for calcium in olivine, all elemental analyses for olivine, orthopyroxene, clinopyroxene, and spinel were carried out under normal analytical conditions; 15 kV acceleration voltage, 15 nA beam current with 2–3 μm beam size. Ferric iron concentrations in pyroxene and spinel were calculated using stoichiometric constraints and assuming that iron is the only element present with variable valency and that oxygen is the only anion (Droop, 1987). Calcium contents in olivine were determined by the following analytical conditions; 20 kV acceleration voltage, 100 nA beam current with 2–3 μm beam size, and 150 s counting intervals conducted simultaneously with three spectrometers. To evaluate the analytical precision, a San Carlos olivine crystal, donated by the Colorado School of Mines Museum, was used as an internal standard (Kil, 2002). The resulting counting precision for EMPA major element measurements is ±0.5%.

About 100 mg of clinopyroxene separates were analyzed for trace and rare earth elements by ICP-MS (VG Elemental Ltd, PQ3) and ICP-AES (Perkin Elmer, Optima 4300DU) at the Korea Basic Science Institute (KBSI) at Daejeon, South Korea. Determinations for USGS reference samples (BIR-1, G-2 and MAG-1) agree with recommended values within suggested tolerances. The precision of the measurement by repeated analyses of reference samples was better than ±5% for major elements and better than ±10% for trace elements.

About 500 mg of clinopyroxenes separates were washed in 10% HCl, 2% HNO_3, and 1% HF and repeatedly rinsed with deionized water in the ultrasonic bath for isotopic analyses. Sr and Nd isotope compositions were measured on a thermal ionization mass spectrometer (VG Sector 54-30) in dynamic mode at the Korean Basic Science Institute. $^{87}Sr/^{86}Sr$ and $^{143}Nd/^{144}Nd$ ratios were normalized to $^{86}Sr/^{88}Sr = 0.1194$ and $^{146}Nd/^{144}Nd = 0.7219$, respectively. The replicate analysis of NBS 987 and La Jolla gave $^{87}Sr/^{86}Sr = 0.710192 \pm 0.000009$ ($2\sigma_m$, $N = 5$) and $^{143}Nd/^{144}Nd = 0.511816 \pm 0.000003$ ($2\sigma_m$, $N = 5$), respectively. Rb, Sr, Sm and Nd concentrations were determined by the isotope dilution technique using ^{87}Rb, ^{86}Sr, ^{149}Sm, and ^{150}Nd as spike solution. Total blank levels were 41 ng for Sr and 12 ng for Nd.

3. Petrography

The spinel lherzolite xenoliths used in chemical analyses were selected from a larger sample collection primarily on the basis of their lack of secondary alteration and absence of evidence for reaction with the host basalt. On the basis of modal composition, all the investigated samples from Boeun fall within the spinel lherzolite field (Fig. 2). These ultramafic xenoliths are commonly composed of olivine,

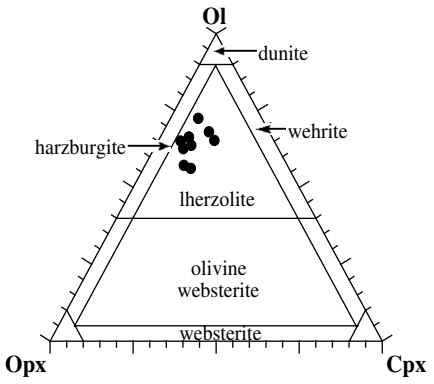

Fig. 2. Modal composition of spinel lherzolites from Boeun. Ol, olivine; Opx, orthopyroxene; Cpx, clinopyroxene.

orthopyroxene, clinopyroxene, and spinel without hydrous minerals, such as phologpite and amphibole.

Following the classification schemes of Mercier and Nicolas (1975) and Harte (1977), ultramafic xenoliths can be classified into three textural types based on the degree of deformation: (a) coarse-grained (> 1 mm) protogranular texture; (b) porphyroclastic texture (with over 50% small polygonal neoblasts); and (c) fine-grained (< 1 mm) equigranular texture that is completely recrystallized. Mercier and Nicolas (1975) considered that the sequence of textures from protogranular through porphyroclastic to equigranular, is related to increasing degree of shear deformation. Spinel lherzolites from Boeun are characterized by protogranular transitional to porpyroclastic textures. Olivines commonly display undulatory extinction and kink banding with curved or straight grain boundaries. Neoblastic olivine and orthopyroxene are polygonal with straight grain boundaries and triple junctions. Orthopyroxene grains display deformation textures similar to olivine crystals, including exsolution lamellae of clinopyroxene. Clinopyroxene and spinel grains are usually less than 1 mm in diameter and do not form porphyroclasts. The boundaries between xenoliths and host basalt are sharp.

4. Mineral chemistry

The mineral chemistry data is listed in Tables 1 and 2. Major element compositions of olivines are homogeneous with forsterite contents ranging from 89.1 to 90.3, which fall within the 'primitive mantle' range (Glücklich and Mercier, 1989).

Orthopyroxenes and clinopyroxenes are classified as enstatite and diopside, respectively, and are characterized by narrow Mg–Fe–Ca ranges from $En_{88}Fs_{10}Wo_1$ to $En_{89}Fs_{11}Wo_3$ and from $En_{46}Fs_5Wo_{48}$ to $En_{48}Fs_6Wo_{48}$, respectively.

Table 1
Representative major element analyses (wt%) of olivine, orthopyroxene, clinopoyroxene, and spinel in spinel lherzolite xenoliths from Boeun

Sample	JC-1				JC-2				JC-3			
	Ol	Opx	Cpx	Sp	Ol	Opx	Cpx	Sp	Ol	Opx	Cpx	Sp
SiO_2	40.41	54.58	51.29	0.03	40.57	54.79	51.44	0.03	40.10	54.57	51.57	0.06
TiO_2	0.01	0.13	0.61	0.05	0.01	0.16	0.58	0.10	0.01	0.12	0.59	0.11
Al_2O_3	0.00	4.64	6.77	59.07	0.04	4.49	7.01	59.13	0.01	4.64	6.74	59.70
Cr_2O_3	0.03	0.40	0.76	9.34	0.01	0.33	0.69	8.58	0.02	0.32	0.61	8.52
FeO	10.29	6.26	2.48	10.39	10.25	6.30	2.71	10.64	10.45	6.78	2.72	10.29
MnO	0.18	0.20	0.11	0.00	0.16	0.14	0.07	0.00	0.11	0.17	0.02	0.00
MgO	49.40	32.98	14.65	20.57	49.53	32.99	14.94	20.90	49.37	32.87	14.79	21.23
CaO	0.04	0.51	21.04	0.01	0.03	0.68	20.11	0.01	0.05	0.63	20.43	0.01
Na_2O	0.01	0.07	1.74	0.02	0.00	0.11	1.86	0.00	0.01	0.11	1.76	0.01
K_2O	0.01	0.02	0.01	0.01	0.00	0.00	0.02	0.00	0.02	0.00	0.00	0.02
Total	100.40	99.80	99.45	99.49	100.59	99.98	99.41	99.41	100.14	100.22	99.23	99.95

Sample	JC-4				JC-5				JC-6			
	Ol	Opx	Cpx	Sp	Ol	Opx	Cpx	Sp	Ol	Opx	Cpx	Sp
SiO_2	40.41	54.52	51.24	0.05	40.27	54.77	51.45	0.06	40.73	55.55	51.40	0.00
TiO_2	0.00	0.14	0.53	0.12	0.01	0.18	0.56	0.07	0.00	0.11	0.50	0.08
Al_2O_3	0.00	4.23	6.91	57.23	0.02	4.70	7.03	58.97	0.00	3.77	5.43	56.09
Cr_2O_3	0.00	0.34	0.92	10.12	0.00	0.28	0.72	9.03	0.02	0.34	0.87	11.99
FeO	10.06	6.75	2.82	11.12	10.37	6.62	3.06	9.74	9.44	6.43	2.19	11.12
MnO	0.09	0.23	0.09	0.00	0.22	0.07	0.02	0.00	0.19	0.18	0.13	0.00
MgO	49.09	33.37	14.67	20.38	48.99	32.91	14.91	21.35	49.38	33.71	15.05	19.99
CaO	0.04	0.59	20.27	0.00	0.04	0.70	19.70	0.00	0.04	0.47	22.49	0.03
Na_2O	0.01	0.09	1.67	0.00	0.07	0.21	1.79	0.00	0.02	0.05	1.22	0.00
K_2O	0.00	0.00	0.02	0.00	0.00	0.01	0.01	0.01	0.00	0.00	0.00	0.02
Total	99.70	100.25	99.14	99.02	99.98	100.45	99.26	99.23	99.82	100.62	99.27	99.32

Sample	JC-7				JC-8				JC-9			
	Ol	Opx	Cpx	Sp	Ol	Opx	Cpx	Sp	Ol	Opx	Cpx	Sp
SiO_2	40.28	54.57	51.62	0.03	40.26	54.12	51.43	0.06	40.14	54.52	51.51	0.05
TiO_2	0.03	0.06	0.33	0.07	0.01	0.20	0.66	0.11	0.04	0.07	0.63	0.05
Al_2O_3	0.04	4.56	6.28	57.70	0.00	4.82	7.05	58.28	0.00	4.39	6.86	59.56
Cr_2O_3	0.00	0.40	0.90	10.39	0.03	0.41	0.78	10.01	0.02	0.29	0.68	8.69
FeO	10.15	6.58	2.56	11.02	9.89	6.13	2.64	10.84	10.59	6.83	2.91	10.17
MnO	0.15	0.17	0.11	0.00	0.13	0.13	0.00	0.00	0.16	0.18	0.08	0.01
MgO	49.07	33.08	14.91	20.49	49.33	32.03	14.55	20.82	48.45	33.03	14.86	20.54
CaO	0.03	0.62	21.08	0.00	0.04	1.52	20.42	0.00	0.04	0.53	20.43	0.01
Na_2O	0.00	0.07	1.56	0.00	0.00	0.21	2.03	0.01	0.01	0.09	1.70	0.01
K_2O	0.00	0.02	0.01	0.01	0.03	0.00	0.03	0.00	0.01	0.00	0.01	0.01
Total	99.77	100.15	99.38	99.71	99.72	99.59	99.59	100.13	99.46	99.95	99.67	99.10

Table 2
Representative trace element contents (ppm) of clinopoyroxene in spinel lherzolite xenolith and host rock (alkali basalt) from Boeun

Sample	Spinel peridotite							Host rock
	JC-1	JC-2	JC-3	JC-4	JC-5	JC-6	JC-7	JC-0
P	60.3	33.8	45.6	34.4	126.8	30.5	181.2	3423.3
Sc	64.1	62.3	61.6	61.9	60.5	68.0	57.8	12.6
V	270.6	260.0	262.1	263.9	263.3	257.3	225.6	232.6
Co	19.4	21.2	21.8	21.1	28.1	19.8	26.6	52.8
Ni	273.6	299.1	310.0	319.1	526.6	299.7	521.1	244.1
Cu	13.4	6.8	9.2	10.9	27.7	9.9	15.2	35.1
Zn	7.45	7.60	7.93	7.78	17.16	7.23	13.80	142.1
Rb	0.99	0.34	0.38	0.30	0.88	0.44	1.24	24.3
Sr	62.6	52.8	61.5	56.1	156.9	53.5	143.6	1066.6
Y	23.0	18.0	19.8	22.0	16.5	19.5	17.8	20.2
Zr	37.5	36.2	33.0	32.3	30.8	29.6	61.8	314.6
Nb	0.47	0.16	0.39	0.40	0.68	0.54	3.13	32.7
Mo	0.10	0.05	0.04	0.05	0.32	0.06	0.37	11.01
Cd	0.14	0.13	0.13	0.16	0.13	0.17	0.16	0.13
Sb	0.05	0.03	0.04	0.03	0.04	0.02	0.04	0.18
Cs	1.44	0.72	1.26	1.07	1.27	0.96	1.35	1.54
Ba	1.39	0.60	1.75	2.43	4.72	2.35	33.59	553.9
La	1.62	0.94	1.18	1.77	7.72	1.37	6.86	49.9
Ce	5.07	3.32	3.99	3.77	14.24	4.15	16.33	96.7
Pr	1.03	0.67	0.78	0.89	1.68	0.79	2.22	11.1
Nd	5.86	3.95	4.47	4.92	6.52	4.31	9.59	42.0
Sm	2.33	1.62	1.84	2.01	1.79	1.72	2.53	8.18
Eu	0.88	0.68	0.74	0.79	0.64	0.69	0.90	2.48
Gd	3.22	2.43	2.77	3.05	2.32	2.64	2.93	6.67
Tb	0.61	0.47	0.51	0.58	0.43	0.50	0.51	0.90
Dy	4.08	3.21	3.46	3.86	2.90	3.40	3.29	4.48
Ho	0.90	0.71	0.78	0.86	0.64	0.76	0.71	0.80
Er	2.72	2.14	2.30	2.55	1.91	2.27	2.06	1.89
Tm	0.39	0.31	0.33	0.37	0.26	0.32	0.30	0.23
Yb	2.43	1.91	2.09	2.23	1.73	2.02	1.84	1.26
Lu	0.36	0.29	0.30	0.33	0.24	0.29	0.28	0.17
Hf	1.33	0.93	0.99	1.10	0.93	1.00	1.44	4.15
Ta	0.04	0.01	0.04	0.06	0.04	0.04	0.17	2.12
Pb	0.24	0.10	0.16	0.16	0.32	0.44	0.45	4.60
Th	0.20	0.10	0.16	0.27	0.82	0.17	0.79	6.14
U	0.03	0.01	0.02	0.02	0.14	0.03	0.22	7.56

Clinopyroxenes are the main carriers of REE, Ti, and Zr among the common minerals of spinel lherzolite, because the M2-sites of orthopyroxene and olivine, as well as octahedral sites of spinel, are significantly smaller than the M2-site of clinopyroxenes (Nagasawa et al., 1980; Stosch, 1982). Typically, the abundances of these elements decrease in the following order: clinopyroxene > orthopyroxene > olivine > spinel. Al_2O_3, Ti, and Y contents in clinopyroxenes decrease with increasing MgO in clinopyroxene (Fig. 3) in spinel lherzolites from Boeun, indicating the possibility of melt extraction (Norman, 1998). In the primitive mantle normalized REE diagram, samples JC-5 and JC-7 are enriched in LREE with $(La/Yb)_N$ ranging from 2.51 to 3.02, but other samples are depleted in LREE with $(La/Yb)_N$ ranging from 0.33 to 0.53 (Fig. 4).

Spinels display a negative relationship between Mg-number $[(Mg)/(Mg + Fe^{2+})]$ and Cr-number $[(Cr)/(Cr + Fe^{3+} + Al)]$ and the observed ranges of Mg-numbers and Cr-numbers of spinels are narrow, ranging from 0.76 to 0.80 and from 0.12 to 0.18, respectively (Fig. 3d). According to the Bergman (1982) classification based on $100(Cr)/(Cr + Al)$ and $100(Mg)/(Mg + Fe^{2+})$, all Boeun xenoliths fall within the field of spinel peridotite xenoliths (Fig. 5).

5. Isotope geochemistry

The Sr and Nd isotopic compositions of clinopyroxenes were analyzed, because Sr and Nd are concentrated in clinopyroxene in spinel lherzolites. The Sr and Nd isotopic data of spinel lherzolites and host basaltic rock from Boeun are shown in Table 3. The $^{87}Sr/^{86}Sr$ and $^{143}Nd/^{144}Nd$ ratios of clinopyroxenes in spinel lherzolites span small ranges; $^{87}Sr/^{86}Sr = 0.702695–0.703346$ ($\varepsilon_{Sr} = -26.3$ to -35.5) and $^{143}Nd/^{144}Nd = 0.512905–0.513161$ ($\varepsilon_{Nd} = 5.2–10.2$). The $^{87}Sr/^{86}Sr$ (0.704319; $\varepsilon_{Sr} = -12.5$) and $^{143}Nd/^{144}Nd$ (0.512850; $\varepsilon_{Nd} = 4.1$) ratios of the host rock (alkali basalt) are higher and lower than those of spinel lherzolites, respectively. The different Sr and Nd isotopic ratios between the host rock and spinel lherzolite xenoliths indicate that the host basaltic rock may have been derived from a different mantle source than the spinel lherzolite.

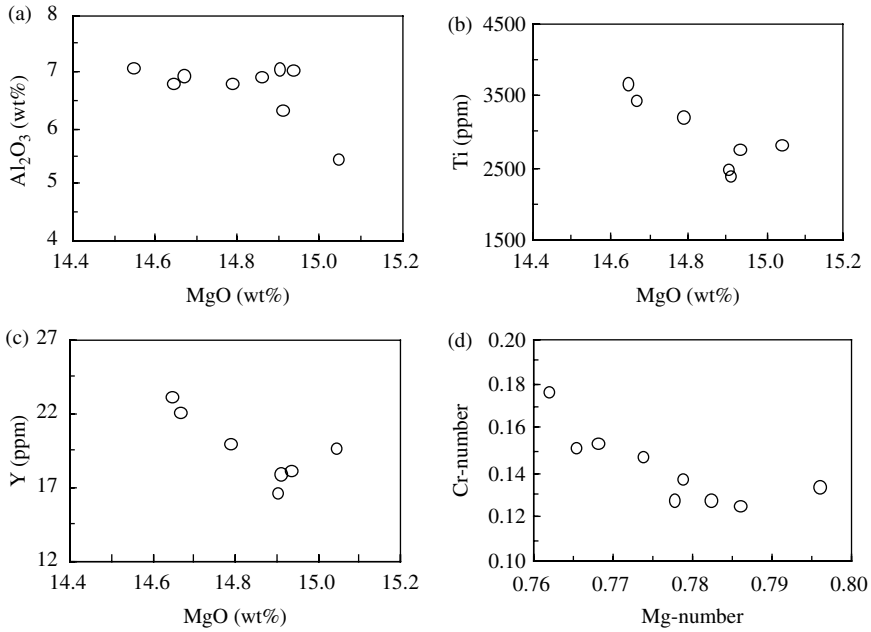

Fig. 3. (a)–(c) MgO vs. Al_2O_3, Ti, and Y contents of clinopyroxenes and (d) Mg-number [(Mg)/(Mg + Fe^{2+})] vs. Cr-number [(Cr)/(Cr + Fe^{3+} + Al)] of spinels in spinel lherzolites from Boeun.

The $^{87}Sr/^{86}Sr$ vs. $^{143}Nd/^{144}Nd$ plots for the host basaltic rock and spinel lherzolites are shown in Fig. 6a. Sr and Nd isotopic compositions show a negative correlation along the mantle array. The Sr and Nd isotopic compositions of spinel lherzolites fall within the MORB (Mid-Ocean Ridge Basalt) field and those of the host basaltic rock fall within the Oceanic Island Basalt field (Fig 6a), indicating that the host basaltic rock may has been derived from a different mantle source. When compared with spinel lherzolites from East China and Southwest Japan, the Sr and Nd isotopic compositions of spinel lherzolites from Boeun are similar to those from East China (Fig. 6b).

6. Equilibrium temperature and pressure conditions

The smooth boundaries between adjacent minerals, the presence of triple junctions, absence of mineral reaction rims, and the uniform compositions of minerals such as olivine, orthopyroxene, and clinopyroxene indicate that equilibrium was reached in the xenoliths prior to basaltic magma eruption.

Two-pyroxene, orthopyroxene, olivine–spinel, and olivine–orthopyroxene-spinel geothermometers were used to calculate the equilibrium temperatures (Table 4). Among them we use the two-pyroxene geothermometers suggested by Wood and Banno (1973), Bertrand and Mercier (1985) and Brey and Köhler (1990). When compared with the Ca-in-orthopyroxene geothermometer suggested by Brey and Köhler (1990), olivine–spinel geothermometer by Ballhaus et al. (1991), and olivine-orthoproxene-spinel geothermometer by Witt-Eickschen and Seck (1991), the Brey and Köhler's (1990) geothermometer provides concordant results with other geothermometers. We believe that the

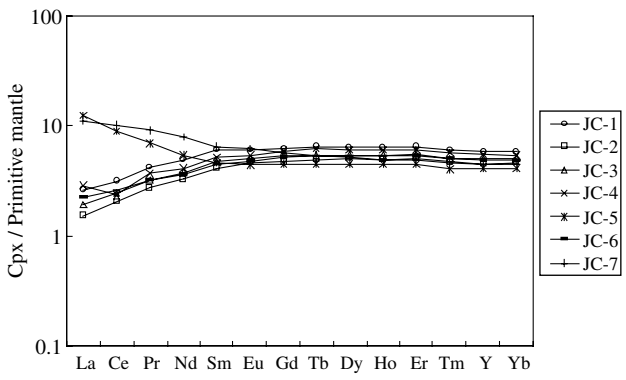

Fig. 4. Primitive mantle-normalized REE patterns of clinopyroxenes from Boeun. Primitive mantle values are from Hofmann (1988).

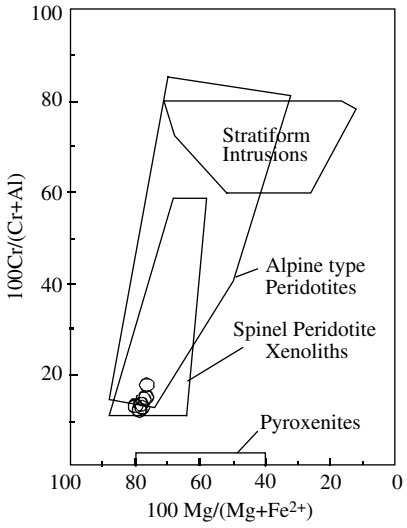

Fig. 5. 100Mg/(Mg + Fe^{2+}) vs. 100Cr/(Cr + Al) for spinels in spinel lherzolites from Boeun (Bergman, 1982).

Table 3
Sr and Nd isotopic ratios and trace element concentrations obtained by isotope dilution technique for spinel lherzolite xenoliths and host rock from Boeun

Sample	Spinel peridotite				Host rock
	JC-1	JC-2	JC-3	JC-6	JC-0
$^{87}Sr/^{86}Sr$	0.703346	0.702695	0.703037	0.702953	0.704319
2σ error	0.000033	0.000033	0.000032	0.000033	0.000032
$^{87}Rb/^{86}Sr$	0.0101	0.0046	0.0048	0.0096	0.0499
Rb (ppm)	0.20	0.09	0.11	0.17	21.97
Sr (ppm)	56.1	57.7	56.0	50.6	1273.3
$^{143}Nd/^{144}Nd$	0.512905	0.513091	0.513063	0.513161	0.512850
2σ Error	0.000057	0.000007	0.000062	0.000066	0.000056
$^{147}Sm/^{144}Nd$	0.2141	0.2397	0.2319	0.2273	0.1137
Sm (ppm)	1.40	1.22	1.15	1.20	7.36
Nd (ppm)	3.95	3.09	2.99	3.20	39.12
Sr/Nd	14.2	18.7	18.7	15.8	32.5
ε_{Sr}	−26.3	−35.5	−30.7	−31.9	−12.5
ε_{Nd}	5.2	8.8	8.3	10.2	4.1
T_{CHUR} (Ma)	2335	1600	1835	2591	

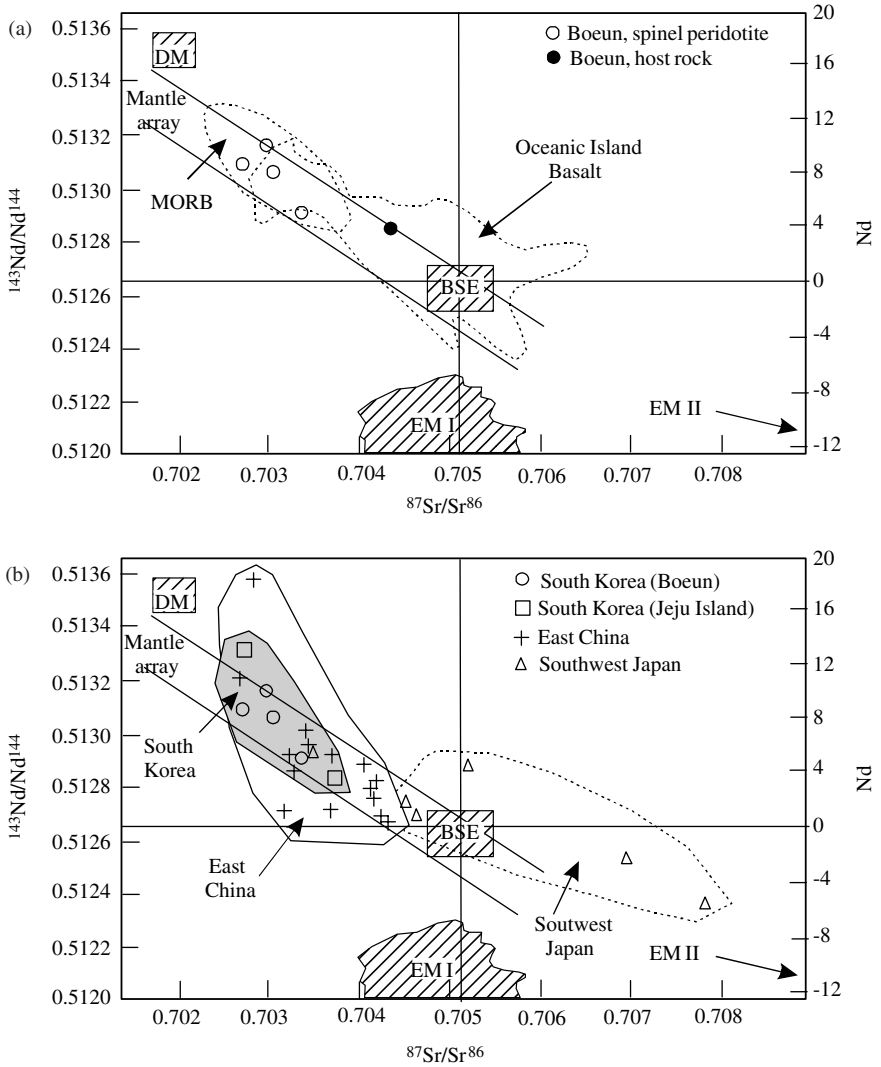

Fig. 6. (a) $^{143}Nd/^{144}Nd$ vs. $^{87}Sr/^{86}Sr$ isotope correlation diagram for clinopyroxenes in spinel lherzolite xenoliths and host rock (alkali basalt). (b) $^{143}Nd/^{144}Nd$ vs. $^{87}Sr/^{86}Sr$ isotope correlation diagram for comparing isotopic compositions of spinel lherzolites in Boeun with those of spinel peridotites in East China and southwest Japan. Oceanic island basalts and hypothetical end-member sources are from Zindler and Hart (1986). Isotopic data for Jeju Island spinel peridotites are from Choi et al. (2002), those for East China (Longgang, Kuandian, Hanluoba, and Minxi areas) are from Xu et al. (2003) and Tatsumoto et al. (1992), and those for southwest Japan (Kurose, Masuda, Noyama-dake, and Tsuyama areas) are from Ikeda et al. (2001). DM, depleted mantle; BSE, bulk silicate earth; and EM, enriched mantle.

Table 4
P–T data for spinel lherzolite xenoliths from Boeun

	JG-1	JG-2	JG-3	JG-4	JG-5	JG-6	JG-7	JG-8	JG-9
T_{WB} (°C) at 15 kb	1027	1082	1056	1077	1106	1026	1048	1064	1072
T_{BM} (°C) at 15 kb	952	1070	1071	1106	1149	945	1015	987	1089
T_{BK} (°C) at 15 kb	847	969	941	986	1030	849	897	902	968
$T_{Ca\text{-}in\text{-}opx}$ (°C) at 15 kb	902	960	942	932	969	880	942	1176	912
T_B (°C) at 15 kb	865	845	892	820	951	799	837	834	900
T_{WS} (°C) at 15 kb	1026	988	988	978	980	963	1022	1049	964
T_{BK} (°C) at P_{KB} (kb)	831	990	938	1012	1056	–	905	900	975
P_{KB} (kb) at T_{BK} (°C)	3.1	29.4	12.8	30.0	29.8	–	20.2	13.2	19.6
P_O (maximum P) (kb)	18.3	18.9	18.7	19.3	19.6	18.9	18.8	18.8	18.9

T_{WB}, Wood and Banno (1973); T_{BM}, Bertrand and Mercier (1985); T_{BK}, Brey and Köhler (1990); $T_{Ca\text{-}in\text{-}Opx}$, Brey and Köhler (1990); T_B, Ballhaus et al. (1991); and T_{WS}, Witt-Eickschen and Seck (1991) geothermometers. P_{KB},Köhler and Brey (1990) geobarometer and P_O, O'Neill (1981) geobarometer (maximum pressure).

Brey and Köhler (1990) geothermometer gives reasonable equilibrium temperature estimation for spinel lherzolites from Boeun. An assumption for the comparison is that blocking temperatures are the same. Accordingly, we suggest that the equilibrium temperatures for spinel lherzolites from Boeun range from 847 to 1030 °C.

The geobarometer suggested by Köhler and Brey (1990), unique for spinel lherzolite, is based on the calcium exchange reaction between olivine and clinopyroxene. Köhler and Brey's (1990) geobarometer was used to determine equilibrium pressures for spinel lherzolites from Boeun (Table 4). Some data points of equilibrium temperature and pressures of spinel lherzolites fall outside of the spinel lherzolite stability field. Similar discrepant results were reported by other researchers (Zipfel and Wörner, 1992; O'Reilly et al., 1997; Medaris et al., 1999; Christensen et al., 2001; Kil and Wendlandt, 2004). A possible explanation of this result is that the Köhler and Brey's (1990) geobarometer is highly dependent on the temperature variations (Kil and Wendlandt, 2004). Therefore, O'Neill's (1981) geobarometer, based on the Cr content of spinel, only provides an upper limit for the equilibrium pressure for spinel lherzolite.

The source depth of spinel lherzolite xenoliths was estimated by Brey and Köhler's (1990) geothermometer, O'Neill's (1981) geobarometer, and heat flow data (Han and Chapman, 1985). The crustal thickness at Boeun, based on seismic velocity, is about 30 km with a corresponding pressure of about 8 kb (Kim and Li, 1998). The heat flow near Boeun is around 74 mW/m^2 (Han and Chapman, 1985). The geothermal gradient at Boeun may be similar to the continental geothermal gradient estimated by Pollack and Chapman (1977), because the 30 km crustal thickness matches the average crustal thickness of the continent and the geothermal gradient of other areas in South Korea is similar to the geothermal gradient of Boeun (Choi et al., 2001). The present geothermal gradient at Boeun may be similar to the paleogeothermal gradient, because there was no major tectonic event from the Miocene to Recent in the Ogcheon tectonic belt. Accordingly, we suggest that spinel lherzolites at Boeun originated at depths from 50 to 63 km (Fig. 7).

7. Discussion

7.1. Element depletion in the xenoliths by melt extraction

Modal compositions and mineral chemistry of spinel lherzolite xenoliths can document the depletion process. In the samples we studied, the clinopyroxene/orthopyroxene ratios decrease with decreasing clinopyroxene abundance since clinopyroxene may be one of the principal

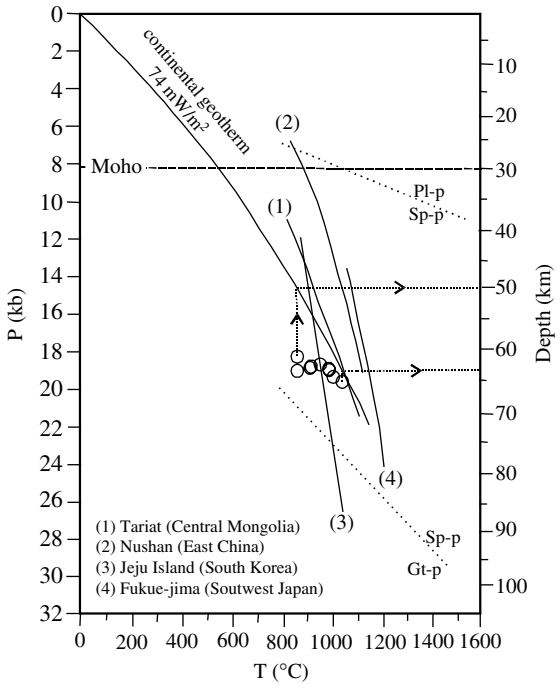

Fig. 7. Temperature versus pressure (depth) conditions for spinel lherzolite xenoliths from Boeun. Temperatures and maximum pressures are calculated using Brey and Köhler's (1990) thermometer and O'Neill's (1981) barometer. The crust thickness is estimated to be 30 km (Kim and Li, 1998). Heat flow at Boeun is 74 mW/m^2 (Han and Chapman, 1985) and the continental geothermal gradient is based on Pollack and Chapman (1977). The geothermal gradients of Tariat, Nushan, Juju Island, and Fukue-jima geothermal lines are from Ionov et al. (1998), Xu et al. (1998), Choi et al. (2001) and Umino and Yoshizawa (1996), respectively. Pl-p, Sp-p, and Gt-p are plagioclase, spinel, and garnet peridotites, respectively.

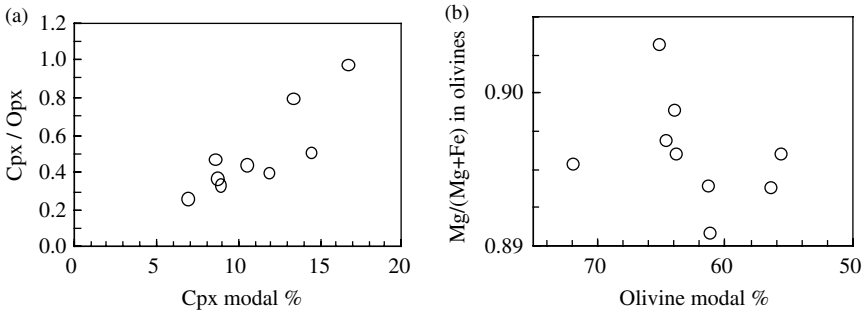

Fig. 8. (a) Modal percentage of clinopyroxene vs. modal Cpx/Opx ratio. (b) Modal percentage of olivine vs. Mg/(Mg + Fe) of olivines in spinel lherzolites from Boeun. Opx, orthopyroxene; Cpx, clinopyroxene.

minerals melted during partial melting of mantle material to produce basaltic magmas (Fig. 8a). Modal percentages of olivine increase with melt extraction and Mg is more enriched than Fe in residual olivine and other major minerals in spinel lherzolite because Mg is relatively refractory. Therefore, increasing modal percentages of olivine with increasing Mg/(Mg + Fe) in olivine strongly suggest that basaltic magma extraction caused the depletion of mantle material beneath Boeun (Fig. 8b). The depletion of Al_2O_3, Ti, and Y with increasing MgO in clinopyroxene (Fig. 3) provides other evidence for melt extraction (Norman, 1998).

The rare earth elements in clinopyroxene were used to model batch and fractional melting. Batch melts remain in equilibrium with the residual solid until segregation, whereas fractional melts are continuously removed as soon as they form (Wilson, 1989). This approach recognizes that clinopyroxene dominates most bulk distribution coefficients for incompatible elements in spinel lherzolite (Kelemen et al., 1993; Halliday et al., 1995; Norman, 1998; Shi et al., 1998). The equations for batch melting and fractional melting we used are from Norman (1998). We used the initial bulk composition of the source, i.e. primitive mantle values from Hofmann (1988) and the fraction of clinopyroxene in primitive mantle spinel lherzolite was assumed to be 0.2 (Fig. 8a). In Fig. 9a, $(Ce/Sm)_N$ vs. $(Ce)_N$ diagrams show that spinel lherzolites deviate slightly from the fractional melting model. Calculations based on fractional melting indicate that spinel lherzolites from Boeun have undergone 1–2% of partial melting (Fig. 9a). Based on primitive mantle-normalized REE patterns for clinopyroxene, spinel lherzolites from Boeun also show 1–2% fractional melting (Fig. 9b). We suggested that the SCLM beneath Boeun had undergone very small degrees of partial melting. Partial melting and extraction of basaltic components from mantle material may have occurred several times after the 2.6 Ga model age, as discussed later.

7.2. Element enrichment in the xenoliths by mantle metasomatism

Mantle metasomatism generally refers to an enrichment process involving incompatible elements, e.g. K, Rb, Sr, Ba, LREE (light rare earth elements), Ti, Nb, Zr, P, U, and Th (Roden and Murthy, 1985; Dawson, 2004). Mantle metasomatism can be subdivided into two types (Dawson, 1984): (1) patent metasomatism (modal metasomatism) which is characterized by mineralogic changes, including introduction of hydrous (amphibole, phlogopite) and/or anhydrous minerals (zircon, apatite, rutile, crichtonite-series minerals); and (2) cryptic metasomatism which is characterized by compositional enrichment without the introduction of new minerals. Two spinel lherzolites (JC-5 and JC-7) display enriched incompatible element patterns

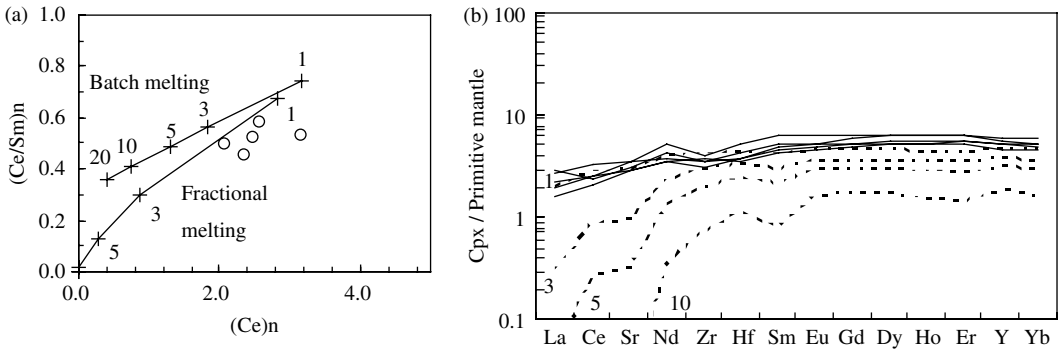

Fig. 9. (a) Partial melting models based on $(Ce)_N$ vs. $(Ce/Sm)_N$ plots of clinopyroxenes in spinel lherzolites from Boeun. Solid line indicates batch melting (1–20%), and dashed line indicates fractional melting (1–5%). (b) Comparison of trace element compositions predicted for residual clinopyroxene having undergone fractional melting (1, 3, 5, 10%; dashed lines) with observed primitive mantle-normalized clinopyroxene compositions.

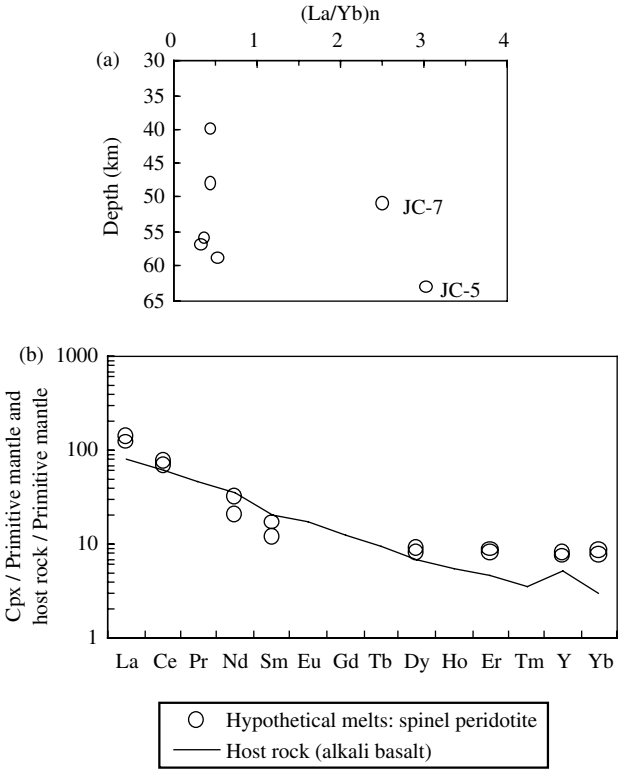

Fig. 10. (a) Primitive mantle-normalized $(La/Yb)_N$ ratios in clinopyroxenes vs. depth (km), (b) REE patterns of hypothetical melt and host rock (alkali basalt) at Boeun $D_{Cpx/Basaltmelt}$ at 1285 °C and 10 kb from Johnson and Schwab (2004) were used to calculate the hypothetical melts. Normalized primitive mantle values are from Hofmann (1988).

without mineralogic changes (Figs. 5 and 10a). This indicates that cryptic metasomatism may have occurred in the SCLM beneath Boeun. In Fig. 10a, primitive mantle-normalized $(La/Yb)_N$ ratios of clinopyroxene do not display any correlation with depth. It indicates that mantle heterogeneity may exist in the SCLM beneath Boeun.

Metasomatic agents in the SCLM beneath Boeun are generally considered to be of three types: silicate magma, carbonatite magma, and H_2O–CO_2 fluid. Carbonatite metasomatism usually results in distinctive petrographic and bulk geochemical changes primarily involving clinopyroxene. Wehrlite xenoliths, produced by interaction between carbonatite magma and upper mantle materials (Yaxley et al., 1991), have not been reported from Boeun, and there are no known carbonatite occurrences near the Boeun area. Wyllie (1977) and Menzies et al. (1985) have argued that large amounts of CO_2 can be released by basaltic and other alkalic magmas at low pressure. CO_2-rich fluids associated with silicate melts have been shown to strongly fractionate LREE (Wendlandt and Harrision, 1979), suggesting a mechanism for LREE-enrichment by CO_2-rich fluids. However, Hamilton et al. (1989) suggest an alterative interpretation that REEs are preferentially partitioned into the silicate melt. In addition, Menzies and Hawkesworth (1987) concluded that melt is a more efficient metasomatic agent than fluids, because the high reactivity of H_2O–CO_2 fluids in hydration and carbonation reactions and partial melting limits fluid mobility.

In Fig 10b, REE compositions of two enriched clinopyroxenes (JC-5 and JC-7) were used to identify the silicate magma metasomatism. Assuming that metasomatic enrichment was caused by entrapment of metasomatizing silicate melt reacting with primary lherzolite minerals in equilibrium, trace element distribution coefficients between clinopyroxene and silicate melt can be used to identify compositional attributes of the metasomatic agent. Concentrations of components in the hypothetical silicate melt are determined using the following equation

$$C_{\text{Silicate melt}} = C_{\text{Cpx}}/D_{\text{Cpx}}/\text{Silicate melts}$$

where $C_{\text{Silicatemelt}}$ and C_{Cpx} are concentrations of an element in the hypothetical silicate melt and clinopyroxene, and $D_{\text{Cpx/Silicatemelt}}$ is the distribution coefficient for an element between clinopyroxene and silicate melt.

The silicate melt compositions are calculated using distribution coefficients between clinopyroxene and basaltic melt ($D_{\text{Cpx/alkalibasaltmelt}}$) because the host rock at Boeun is alkali basalt. The distribution coefficient values (D) are controlled by pressure, temperature, and bulk chemistry. We used $D_{\text{Cpx/Alkalibasaltmelt}}$ values from Johnson and Schwab (2004) for upper mantle conditions of 1285 °C and 10 kb. Subsequently, the REE contents of the hypothetical (calculated) silicate melt were compared with actual host rock analyses (alkali basalt) to test whether the model is correct. In Fig. 10b, the calculated REE patterns for the hypothetical silicate melt agree well with the host rock compositions. Beccaluva et al. (2001) suggested that complete chemical rehomogenization of a 1 mm clinopyroxene requires a time span of 4.8–16 ka, based on diffusion models for clinopyroxene. Therefore, we suggest that the metasomatic agent for the enriched spinel lherzolites at Boeun may be an alkali basaltic magma that preceded the entrainment of ultramafic xenoliths by the host magma and/or previous alkali basaltic magma.

7.3. Characteristics of subcontinental lithospheric mantle (SCLM)

The Sr/Nd ratios (10.7–24.1) of clinopyroxenes in spinel lherzolites from Boeun are similar to Sr/Nd ratios (20–30) of clinopyroxenes in spinel peridotites from East China, San Carlos, Eifel and Tariat Depression (Stosch and Lugmair, 1986; Stosch et al., 1986; Zindler and Jagoutz, 1988; Song and Frey, 1989), but are different from the ratios (mostly < 10) of clinopyroxenes in spinel peridotites from Japanese Island Arcs (Abe et al., 1998). In Fig. 6b, $^{87}Sr/^{86}Sr$ and $^{143}Nd/^{144}Nd$ isotope ratios of clinopyroxenes in spinel lherzolites from Boeun are similar to those of clinopyroxenes in spinel peridotites from East China, but are different from those of clinopyroxenes in spinel peridotites from Southwest Japan, which have higher $^{87}Sr/^{86}Sr$ and lower $^{143}Nd/^{144}Nd$ ratios, indicating that the SCLM composition represented by the spinel lherzolites from Boeun

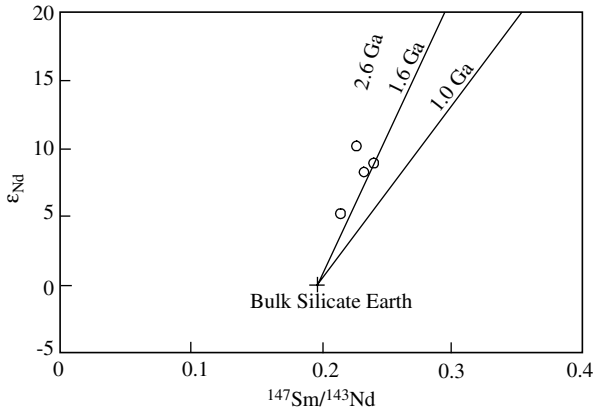

Fig. 11. ε_{Nd} vs. $^{147}Sm/^{144}Nd$ isotopic evolution diagram of spinel lherzolites from Boeun. Sm–Nd ages are calculated with $\lambda = 6.54\times10^{-12}$ yr^{-1} and the present-day Bulk Silicate Earth values are $^{147}Sm/^{144}Nd = 0.1967$ and $^{147}Nd/^{144}Nd = 0.512638$ (Jacobsen and Wasserburg, 1980).

may have not been affected by subduction of the Western Pacific margin.

The model age indicates the initial separation time from the upper mantle. The Sm and Nd isotopic compositions, rather than Rb and Sr isotopic compositions, are usually used to determine the model age because secondary processes may change the Sr isotopic composition. The spinel lherzolites from Boeun, except for two enriched ones (JC-5 and JC-7), are used to determine the model age. The calculated Nd model ages for spinel lherzolites using a single stage model are between 1.6 and 2.6 Ga, indicating a late Archean to early Proterozoic age (Fig. 11).

The underlying SCLM are approximately the same ages as the overlying crust for most cratons (Wu et al., 2003). There is no reasonable age available for the basement rocks in the Ogcheon belt, but the age of basement rocks in the Gyeonggi massif and the Yeongnam massif near Ogcheon belt are 2.0–1.8 Ga (Sagong et al., 2003). The age spans of the basement rocks fall within the model age of SCLM beneath Boeun. The model ages of SCLM beneath Boeun are also similar to the model age (2.0 Ga) of spinel peridotites from Tariat in central Mongolia and Hannuoba in East China (Stosch et al., 1986; Song and Frey, 1989). Accordingly, the SCLM beneath Boeun was separated sometime between 1.6 and 2.6 Ga.

8. Conclusion

The geochemical data on spinel lherzolite xenoliths from Boeun, Korea, provides important information for the subcontinental lithospheric mantle, such as mantle composition, equilibrium temperature and pressure conditions, and chemical depletion and enrichment processes.

All spinel lherzolite xenoliths found in Boeun have protogranular to porpyroclastic textures. The sharp contact between the host rock (alkali basalt) and spinel lherzolite xenoliths indicate that the spinel lherzolite xenoliths were incorporated into ascending alkali basalt magma.

Using the Brey and Köhler (1990) geothermometer and O'Neill's (1981) geobarometer, together with heat flow-derived geothermal gradients, were estimated the equilibrium temperature and extraction depths to be 847–1030 °C and 50–63 km, respectively.

The decrease in clinopyroxene/orthopyroxene ratios with decreasing clinopyroxene content, and the decrease of Al_2O_3, Ti, and Y contents with increasing MgO in the clinopyroxenes, suggest that basaltic melt extraction has occurred. Fosterite contents of olivines, Mg–Fe–Ca ranges of pyroxenes, Cr-numbers of spinels, and REE composition of clinopyroxenes indicate that the SCLM beneath Boeun may have undergone small degrees (1–2%) of fractional melting.

Some enriched spinel lherzolite from Boeun may have undergone cryptic metasomatism caused by an alkali basaltic melt. $(La/Yb)_N$ ratios of clinopyroxene in the enriched and depleted spinel lherzolites are different and do not show variations with depth. These indicate a heterogeneous SCLM beneath the Boeun area. The model age (1.6–2.6 Ga) of spinel lherzolite xenoliths is similar to the age of the basement rocks (2.0–1.8 Ga) near Boeun and those of East China and Central Mongolia.

Acknowledgements

I am grateful to Dr Seok-Hoon Lee, Chang-Sik Cheong, Hyeong-Sun Sin, and Youn-Joong Jeong of Korea Basic Science Institute for analyzing mineral and isotopic compositions. I would like to thank Dr Yigang Xu and anonymous reviewer for leading to significant improvements of the manuscript.

References

Abe, N., Arai, S., Yurimoto, H., 1998. Geochemical characteristics of the uppermost mantle beneath the Japan island arcs: implications for upper mantle evolution. Physics of the Earth and Planetary Interiors 107, 233–248.

Ballhaus, C., Berry, R.F., Green, D.H., 1991. High pressure experimental calibration of the olivine-orthopyroxene-spinel oxygen geobarometer: implications for the oxidation state of the upper mantle. Contributions to Mineralogy and Petrology 107, 27–40.

Beccaluva, L., Bonadiman, C., Coltorti, M., Salvini, L., Siena, F., 2001. Depletion event, nature of metasomatizing agent and timing of enrichment processes in lithospheric mantle xenoliths from the veneto volcanic province. Journal of Petrology 42, 173–187.

Bergman, S.C., 1982. Petrogenetic aspects of the alkali basaltic lavas and included megacrysts and nodules from the Lunar Crater volcanic field, Nevada, USA. PhD thesis, Princeton University, New Jersey, p. 447.

Bertrand, P., Mercier, J.C.C., 1985. The mutual solubility of coexisting ortho- and clinopyroxene: toward an absolute geothermometer for the natural system? Earth and Planetary Science Letters 76, 109–122.

Bonatti, E., Ottonello, G., Hamlyn, P.R., 1986. Lherzolites from Island of Zabargad (St John) Red Sea: petrology and geochemistry. Journal of Geophysical Research 91, 599–631.

Brey, G.P., Köhler, T., 1990. Geothermobarometry in four-phase lherzolites II. new thermobarometers, and practical assessment of existing thermobarometers. Journal of Petrology 31, 1353–1378.

Choi, S.-H., 2000. Oxidation state of mantle xenoliths from Jeju-do, South Korea. Geoscience Journal 4, 211–220.

Choi, S.-H., Jwa, Y.-J., Lee, H.-Y., 2001. Geothermal gradient of the upper mantle beneath Jeju Island, Korea: evidence from mantle xenoliths. The Island Arc 10, 175–193.

Choi, S.-H., Lee, J.-I., Park, C.-H., Moutte, J., 2002. Geochemistry of lherzolite xenoliths in alkali basalts from Jeju Island, Korea. The Island Arc 11, 221–235.

Chough, S.K., Kwon, S.T., Ree, J.H., Choi, D.K., 2000. Tectonic and sedimentary evolution of the korean peninsula: a review and new view. Earth-Science Review 52, 175–235.

Christensen, N.I., Medaris, L.G., Wang, H.F., 2001. Depth variation of seismic anisotropy and petrology in central European lithosphere: a tectonothermal sysnthesis from spinel lherzolite. Journal of Geophysical Research 106, 645–664.

Cluzel, D., Lee, B.J., Cadet, J.P., 1991. Indosinian dextral ductile fault system and synkinematic plutonism in the southwest of the Ogcheon belt (South Korea). Tectonophysics 194, 131–151.

Dawson, J.B., 1984. Contrasting types of upper mantle metasomatism? In: Kornprobst, J. (Ed.), Kimberlites II. Elsevier, Amsterdam, pp. 289–294.

Dawson, J.B., 2004. A fertile harzburgite–garnet lherzolite transition: possible inferences for the roles of strain and metasomatism in upper mantle lherzolites. Lithos 77, 553–569.

Droop, G.T.R., 1987. A general equation for estimating Fe^{3+} concentrations in ferromagnesian silicates and oxides from microprobe analyses, using stoichiometric criteria. Mineralogical Magazine 51, 431–435.

Glücklich, M.E., Mercier, J.C.C., 1989. The basin-and-range lithospheric mantle: evidence for homogeneity at the regional scale. TERRA Abstract 1, 318.

Halliday, A., Lee, D.-C., Tommasini, S., Davies, G.R., Paslick, C.R., Fitton, J.G., James, D.E., 1995. Incompatible trace elements in OIB and MORB and source enrichment in the sub-oceanic mantle. Earth and Planetary Science Letters 133, 379–395.

Hamilton, D.L., Bedson, P., Esson, J., 1989. The behavior of trace element in the evolution of carbonatites. In: Bell, K. (Ed.), Carbonatites—Genesis and Evolution. Unwin Hyman, Boston, pp. 405–427.

Han, W., Chapman, D.S., 1985. On the regional heat flow around Korea reduced heat flow. Journal of the Geological Society of Korea 21, 74–78.

Harte, B., 1977. Rock nomenclature with particular relation to deformation and recrystallization textures in olivine-bearing xenolith. Journal of geology 85, 279–288.

Ho, K.-S., Chen, J.-C., Smith, A.D., Juang, W.-S., 2000. Petrogenesis of two groups of pyroxenite from Tungchihsu, Penghu Islands, Taiwan Strait: implications for mantle metasomatism beneath SE China. Chemical Geology 167, 355–372.

Hofmann, A.W., 1988. Chemical differentiation of the Earth: the relationship between mantle, continental crust, and oceanic crust. Earth and Planetary Science Letters 90, 297–314.

Ikeda, Y., Nagao, K., Kagami, H., 2001. Effects of recycled materials involved in a mantle source beneath the southwest Japan arc region: evidence from noble gas, Sr, and Nd isotopic systematics. Chemical Geology 175, 509–522.

Ionov, D.A., O'Reilly, S.Y., Griffin, W.L., 1998. A geotherm and lithspheric section for central Mongolia (Tariat Region). In: Flower, M.F.J., Chung, S.L., Lo, C.H., Lee, T.Y. (Eds.), Mantle Dynamics and Plate Interactions in East Asia. American Geophysical Union, Washington, DC, pp. 127–153.

Jacobsen, S.B., Wasserburg, G.J., 1980. Sm–Nd evolution of chondrites. Earth and Planetary Science Letters 50, 139–155.

Johnson, A.D., Schwab, B.E., 2004. Constraints on clinopyroxene/melt partitioning of REE, Sr, Ti, Cr, Zr, and Nb during mantle melting: first insights from direct lherzolite melting experiments at 1.0 Gpa. Geochimica et Cosmochimica Acta 68, 4949–4962.

Kelemen, P., Shimizu, N., Dunn, T., 1993. Relative depletion of niobium in some magmas and the continental crust: partitioning of K, Nb, La and Ce during melt/rock reaction in the upper mantle. Earth and Planetary Science Letters 120, 111–134.

Kil, Y., 2002. Mantle Evolution associated with the Rio Grande Rift: geochemistry and geothermobarometry of upper mantle xenoliths. PhD thesis, Colorado School of Mines, Golden, p. 160.

Kil, Y., Wendlandt, R.F., 2004. Pressure and temperature evolution of upper mantle under the Rio Grande Rift. Contributions to Minieralogy and Petrology 148, 265–280.

Kim, S.G., Li, Q., 1998. 3-D crustal velocity tomography in the Southern part of the Korean peninsula. Journal of Korea Society of Economic and Environmental Geology 31, 127–139.

Kim, Y.K., Lee, D.S., Song, Y.K., Kim, S.E., 1988. Petrology of ultramafic nodules in Jogok-ri basalt, Boun Area. Journal of the Geological Society of Korea 24, 57–66 (in Korean with English abstract).

Kim, K.H., Nagao, K., Tanaka, T., Sumino, H., Nakamura, T., Okuno, M., Ishitsuka, Y., Jin, B.L., Song, J.H., 2004. He–Ar and Nd–Sr isotopic compositions of ultramafic xenoliths and host alkali basalts from the Korean peninsula. Annual meeting of the Korea Society of Economic and Enviromental Geology, 125.

Köhler, T.P., Brey, G.P., 1990. Calcium exchange between olivine and clinopyroxene calibrated as a geothermobarometer for natural lherzolites from 2 to 60 kb with applications. Geochimica et Cosmochimica Acta 54, 2375–2388.

Lee, H.Y., 2002. Petrology of spinel lherzolite from South Korea: implication of P/T estimate. International Geology Review 38, 320–325.

Maaløe, S., Aoki, K., 1977. The major element composition of upper mantle estimated from the composition of lherzolites. Contributions to Mineralogy and Petrology 63, 161–173.

Medaris, G.L., Wang, H.F., Fournelle, J.H., Zimmer, J.H., Jelinek, E., 1999. A cautionary tale of spinel lherzolite thermobarometry: an example from xenoliths of Kozákov Volcano, Czech republic. Geolines 9, 92–96.

Menzies, M.A., Hawkesworth, C.J., 1987. Mantle metasomatism. Academic Press, London, p. 472.

Menzies, M., Kempton, P., Dungan, M., 1985. Interaction of continental lithosphere and asthenospheric melts below the Geronimo volcanic field, Arizona, USA. Journal of Petrology 26, 663–693.

Mercier, J.C., Nicolas, A., 1975. Texture and fabrics of upper mantle lherzolites as illustrated by xenoliths from basalts. Journal of Petrology 16, 454–487.

Nagasawa, H., Schreiber, H.D., Morris, R.V., 1980. Experimental mineral/liquid partition coefficients of the rare earth elements (REE), Sc and Sr for perovskite, spinel and melilite. Earth and Planetary Science Letters 46, 431–437.

Nixon, P.H., 1987. Mantle xenoliths. Wiley, New York, p. 844.

Norman, M.D., 1998. Melting and metasomatism in the continental lithosphere: laser ablation ICPMS analysis of minerals in spinel lherzolites from eastern Australia. Contributions to Mineralogy and Petrology 130, 240–255.

O'Neill, H.St.C., 1981. The transition between spinel lherzolite and garnet lherzolite, and its use as a geobarometer. Contributions to Mineralogy and Petrology 77, 185–194.

O'Reilly, S.Y., Chen, D., Griffin, W.L., Ryan, C.G., 1997. Minor elements in olivine from spinel lherzolite xenoliths: implications for thermobarometry. Mineralogical Magazine 61, 257–269.

Pollack, H.N., Chapman, D.S., 1977. On the regional variation of heat flow, geotherms and lithospheric thickness. Tectonophysics 38, 279–296.

Roden, M.F., Murthy, V.R., 1985. Mantle metasomatism. Annual Review of Earth and Planetary Sciences 13, 269–296.

Sagong, H., Cheong, C.-S., Kwon, S.-T., 2003. Paleoproterozoic orogeny in South Korea: evidence from Sm–Nd and Pb step-leaching garnet ages of precambrian basement rocks. Precambrian Research 122, 275–295.

Shi, L., Francis, D., Ludden, J., Frederiksen, A., Bostock, M., 1998. Xenolith evidence for lithospheric melting above anomalously hot mantle under the northern Canadian Cordillera. Contributions to Mineralogy and Petrology 131, 39–53.

Solomon, M., 1963. Counting and sampling errors in modal analysis by point counter. Journal of Petrology 4, 367–382.

Song, Y., Frey, F.A., 1989. Geochemistry of lherzolite xenoliths in basalt from Hannuoba, eastern China: implications for subcontinental mantle heterogeneity. Geochimica et Cosmochimica Acta 53, 97–113.

Stosch, H.G., 1982. Rare earth element partitioning between minerals from anhydrous spinel lherzolite xenoliths. Geochimica et Cosmochimica Acta 46, 793–811.

Stosch, H.G., Lugmair, G.W., 1986. Trace element and Sr and Nd isotope geochemistry of lherzolite xenoliths from the Eifel (Germany) and their bearing on the evolution of the subcontinental lithosphere? Earth and Planetary Science Letters 47, 263–271.

Stosch, H.G., Lugmair, G.W., Kovalenko, V.I., 1986. Spienl lherzolite xenoliths from the Tariat Depression, Mongolia. II. Geochemistry and Nd and Sr isotope composition and their implication for the evolution of the subcontinental lithosphere. Geochimica et Cosmochimica Acta 50, 2601–2614.

Tatsumoto, M., Basu, A.R., Wankang, H., Junwen, W., Guanghong, X., 1992. Nd, Nd, and Pb isotope of ultramafic xenoliths in volcanic rocks of Eastern China: enriched components EMI and EMII in subcontinental lithosphere. Earth and Planetary Science Letters 113, 107–128.

Umino, S., Yoshizawa, E., 1996. Petrology of ultramafic xenoliths from Kishyuku lava, Fukue-jima, southwest Japan. Contributions to Mineralogy and Petrology 124, 154–166.

Wendlandt, R.F., Harrision, W.J., 1979. Rare earth partitioning between immiscible carbonate and silicate liquids and CO_2 vapor: results and implications for the formation of light rare earth-enriched rocks. Contributions to Mineralogy and Petrology 69, 409–419.

Wilson, M., 1989. Igneous petrogenesis. Unwin Hyman, Boston, p. 466.

Witt-Eickschen, G., Seck, H.A., 1987. Temperature of sheared mantle xenoliths from the West Eifel, West Germany: evidence for mantle diapirism beneath the rhenish massif. Journal of Petrology 28, 475–493.

Witt-Eickschen, G., Seck, H.A., 1991. Solubility of Ca and Al in orthopyroxene from spinel lherzolite: an improved version of an empirical geothermometer. Contributions to Mineralogy and Petrology 106, 431–439.

Wood, B.J., Banno, S., 1973. Garnet-orthopyroxene and orthopyroxene–clinopyroxene relationships in simple and complex systems. Contributions to Mineralogy and Petrology 42, 109–124.

Wu, F., Walker, R., Ren, X., Sun, D., Zhou, X., 2003. Osmium isotopic constraints on the age of lithospheric mantle beneath northeastern China. Chemical Geology 196, 107–129.

Wyllie, P.J., 1977. Mantle fluid composition buffered in lherzolite–CO_2–H_2O by carbonates, amphibole and phlogopite. Journal of Geology 86, 687–713.

Xu, X., O'Reilly, S.Y., Griffin, W.L., Zhou, X., Huang, X., 1998. The nature of the cenozoic lithosphere at Nushan. In: Flower, M.F.J., Chung, S.L., Lo, C.H., Lee, T.Y. (Eds.), Mantle Dynamics and Plate Interactions in East Asia. American Geophysical Union, Washington, pp. 167–195.

Xu, Y., Menzies, M.A., Thirlwall, M.F., Huang, X., Liu, Y., Chen, X., 2003. Reactive harzburgites from huinan, NE China: products of the lithosphere–ashtenosphere interaction during lithospheric thinning? Geochimica et Cosmochimica Acta 67, 487–505.

Yaxley, G.M., Crawford, A.J., Green, D.H., 1991. Evidence for carbonatite metasomatism in spinel lherzolites from western Victoria Australia. Earth and Planetary Science Letters 197, 305–317.

Zindler, A., Hart, S.R., 1986. Chemical geodynamics. Annual Review of Earth and Planetary Science Letters 14, 497–571.

Zindler, A., Jagoutz, E., 1988. Mantle cryptology. Geochimica et Cosmochimica Acta 52, 319–333.

Zipfel, J., Wörner, G., 1992. Four- and five-phase lherzolites from a continental rift system: evidence for upper mantle uplift and cooling at the Ross Sea margin (Antarctica). Contributions to Mineralogy and Petrology 111, 24–36.